Available online at www.sciencedirect.com

ScienceDirect

Materials Today: Proceedings 5 (2018) 22412–22420

materialstoday: PROCEEDINGS

www.materialstoday.com/proceedings

ICASE_2017

Novel $NiWO_4$-ZnO-NRGO Ternary Nanocomposites With Enhanced Photocatalytic Activity

M. Mohamed Jaffer Sadiq, D. Krishna Bhat*

National Institute of Technology Karnataka, Surathkal, Mangalore-575025, Karnataka, India.

Abstract

A novel $NiWO_4$-ZnO-NRGO ternary nanocomposite was efficiently synthesized via a facile, fast and easy microwave irradiation technique and its capability to photodegrade organic dye in aqueous solution was investigated. The products were characterized through X-ray diffraction (XRD), field emission scanning electron microscopy (FESEM), transmission electron microscopy (TEM), high resolution transmission electron microscopy (HRTEM), Raman spectroscopy, photoluminescence spectroscopy (PL), X-ray photoelectron spectroscopy (XPS) and diffuse reflectance spectroscopy (DRS) techniques. The photocatalytic activity was evaluated by estimating the extent of photodegradation of methylene blue (MB) under irradiation of visible light source, which showed 9 times enhancement for the ternary composites compared to that for pure $NiWO_4$. The outcomes reveal that the novel $NiWO_4$-ZnO-NRGO ternary nanocomposite could be a highly efficient visible light photocatalyst for the removal of environmental contaminants in wastewater.

Selection and/or Peer-review under responsibility ofInternational Conference on Advances in Science & Engineering ICASE - 2017.

Keywords:$NiWO_4$-ZnO-NRGO nanocomposite; photocatalytic activity; microwave irradiation technique; wastewater treatment; dye degradation.

1. Introduction

In last few decades, water pollution due to industrial effluents has become a huge concern for the environment [1]. Waste water released from various industries containing toxic chemicals has posed a threat to aquatic as well as human life. In such a situation development of new strategies for environmental remediation is the need of the day. Photocatalysis has emerged as a savior in this respect. Nanoparticles like ZnO, NiO, TiO_2, Fe_3O_4, Co_3O_4 and their composites show a great promise as photocatalysts due to their excellent physical and chemical properties [2-6].

* Corresponding author. Tel.: +91-824-2473202; fax: +91-824-74033/2474082.
*E-mail address:*denthajekb@gmail.com

Selection and/or Peer-review under responsibility ofInternational Conference on Advances in Science & Engineering ICASE - 2017.

Likewise, metal tungstates have also attracted attention due to their band gap tunability when coupled with other semiconductors [7,8]. Reduced graphene oxide (RGO) is a single-atom thick sheet formed by sp^2-bonded carbonatoms packed into a 2D hexagonal lattice. It has desirable properties like large surface area; better chemical and mechanicalstrength;good optical, electrical and thermalproperties [9-12].

In order to achieve excellent catalytic performance in nanocomposites two important factors have to be considered: faster electron transfer and better charge separation. A combination of semiconductors with suitable band gaps can promote charge carrier separation [13]. There are many reports on the incorporation of carbon nanostructures such as graphene and carbon nanotubes as components of photocatalyst composites to enhance the activity [14-19]. The incorporation of nitrogen atoms which are rich in electrons, into RGO promotes the interaction between neighboring carbons atoms and electrons. NRGO increases the transfer rate of electron from the conduction band(CB) of the semiconductor and also creates an additional donor level above the valence band of semiconductors thereby reducing the energy requirement for the excitation of electron from valance band (VB) to CB of semiconductor materials [20,21]. The ternary composites have better charge carrier separation and a fast electron transfer system compared to the pristine semiconductor materials [22]. However, excellent catalytic performance with high stability and low cost are still rare [23].

In view of the aforementioned facts a novel $NiWO_4$-ZnO-NRGO ternary nanocomposite has been efficiently synthesized via a facile, cost effective microwave irradiation technique. The as-synthesized nanocomposite was characterized by diffraction, microscopic, spectroscopic techniques to study the elemental composition, morphology and optical properties. The photocatalytic efficiency was studied in photodegradation of MB dye in aqueous solution. The ternary composite shows excellent photocatalytic activity, stability and reusability compared to the pristine materials. This photocatalyst shows a huge promise in environmental remediation and industrial application. To the best of our knowledge this is the first report on synthesis and study of photocatalytic activity of $NiWO_4$-ZnO-NRGO ternary composite in degradation of MB.

2. Experimental

2.1 Materials and method

All the reagents and chemicals were obtained from Sigma-Aldrich and were utilized without additional purification. Millipore water was used to carry out all the experiments.

2.2 Preparation of the ternary $NiWO_4$-ZnO-NRGO ternary nanocomposites

GO was prepared by modified Hummers method as reported elsewhere [7, 8]. $NiWO_4$-ZnO-NRGO ternary nanocomposites were synthesized via microwave irradiation method [15]. In a typical synthesis, 0.01 M of nickel acetate solution and 0.01 M of sodium tungstate solution was slowly added to the calculated amount of dispersed GO solution under consistent stirring for approximately 2 hours. During this calculated amount of zinc acetate and sodium hydroxide was also added. The pH of the solution was maintained at 9 using ammonia. Later, 1 % urea was added to the above mixture. The resulting solution was irradiated with microwave (350 W) for 10 minutes and the obtained precipitate was allowed to cool naturally. The precipitate was centrifuged and washed several times with water and ethanol and then finally dried at 80 °C for 12 hours. Control samples containing NRGO, $NiWO_4$, ZnO, $NiWO_4$-NRGO and ZnO-NRGO was also synthesized using the same procedure.

2.3 Characterization

The phase structure and purity of the nanocomposites were investigated using XRD (Rigaku) with Cu-K_α radiation for 2θ range of 5° -60° with a scan rate of 1 °/minute. Raman spectrum was recorded at 532 nm using the laser Raman microscope (Renishaw, Invia) equipped with He-Ne laser source. The morphology of the samples was studied using field emission scanning electron microscope (FESEM, Ultra 55 Zeiss), transmission electron microscope (TEM, Tecnai G20) and high-resolution transmission electron microscope (HRTEM, Tecnai). Elemental

composition was determined using XPS (Kratos XSAM800) equipped with a standard monochromatic Al K_α source. UV-visible spectrum was obtained by diffuse reflectance method (Analytic Jena). The photoluminescence (PL) spectrum was recorded using fluorescence spectrophotometer (Horiba JobinYvon).

2.4 Determination of photocatalytic activity

Photocatalytic properties of the ternary nanocomposites were studied using MB following procedure reported elsewhere [18]. 20 mg of nanocomposites were dispersed in 200 mL aqueous solution of 10 mg/L MB dye and stirred for 30 minutes in the dark to attain adsorption desorption equilibrium. Later, this solution was exposed to a 250 W Hg lamp provided with a cutoff filter of 400 nm. At regular time intervals, 4 mL of the MB solution was withdrawn and centrifuged to remove the residual nanocomposites. The supernatant was used to record the absorbance at 664 nm wavelength. The percentage of photodegradation of the MB dye was calculated using equation (1).

$$\text{Percentage of photodegradation of the MB dye} = [(C - C_o) / C] \times 100 \quad \text{---------} \quad (1)$$

where, C is the initial concentration and C_o is the concentration at a given interval time, of the MB dye solution, respectively.To determine the possible photocatalytic degradation mechanism, trapping experiments were conducted using various kinds of scavengers. In trapping experiments, the photocatalytic activity of the catalyst was determined under similar conditions as outlined above in the presence of a scavenger for a particular species.

3. Results and discussion

3.1 XRD Studies

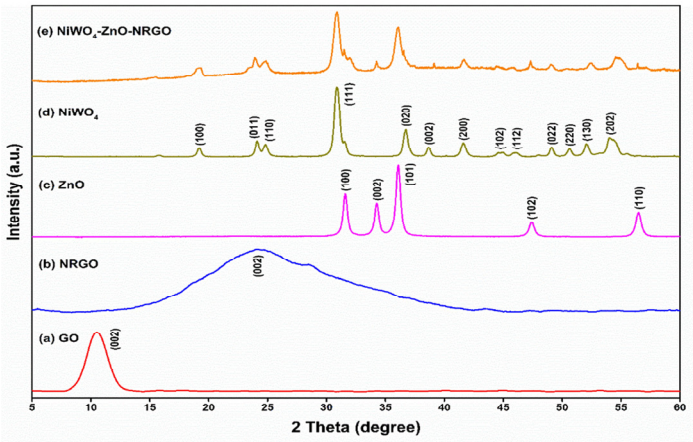

Fig. 1. XRD spectrum of (a) GO, (b) NRGO, (c) $NiWO_4$, (d) ZnO and (e) $NiWO_4$-ZnO-NRGO ternary nanocomposites.

Fig. 1 reveals the XRD patterns of the as-synthesized GO, NRGO, $NiWO_4$, ZnO and $NiWO_4$-ZnO-NRGO. The diffraction peaks at 10.5° corresponds to (002) planes of GO sheets. The diffraction peaks at 22.6° corresponds to (002) planes of NRGO sheets. ZnO diffraction peaks at 31.6°, 34.2°, 36.1°, 47.4°, 56.4°, 62.7°, 66.2°, 67.8° and 68.9° can be indexed to the (100), (002), (101), (102), (110), (103), (200), (112) and (201) as indicated in JCPDS file no. 36-1451. $NiWO_4$ diffraction peaks at 19.2°, 24.1°, 24.8°, 30.9°, 31.5°, 36.7°, 38.7°, 41.6°, 44.9°, 49.1°, 50.6°, 52.0°, 54.2°, 65.2° and 68.6° is ascribed to the (100), (011), (110), (111), (020), (002), (200), (102), (112), (022), (220), (130), (202), (132) and (041) planes according to JCPDS file no. 15-0755. Peaks corresponding to NRGO were not found in the diffraction pattern of ternary composite. This may be due to the small quantity and exfoliated nature of NRGO in the composite [14].

3.2 Raman Studies

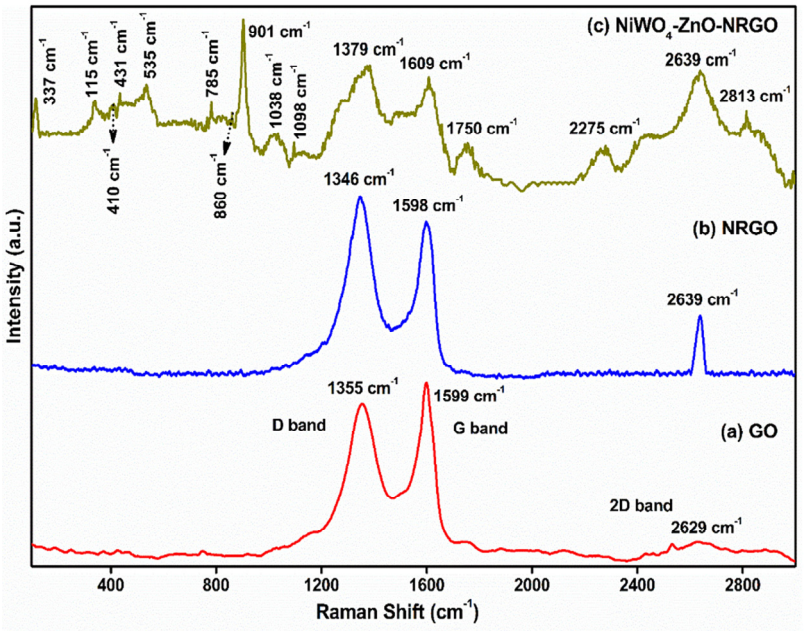

Fig. 2. Raman spectra of (a) GO, (b) NRGO and (c) $NiWO_4$-ZnO-NRGO ternary nanocomposites.

Raman spectrum of GO reveals two distinct modes: G mode at 1599 cm^{-1} and D mode at 1355 cm^{-1}as shown in Fig. 2a. The intensity ratios of D to G band (I_D/I_G) is a measure of relative concentration of sp^3 hybridized defects to sp^2 hybridized GO domains. We see that after microwave irradiation the I_D/I_G ratio increases from 0.87 for GO to 1.09 for the composite indicating the formation of more defects in NRGO (Fig. 2b) during the reduction [17]. Slight variation in the Raman frequency, appearance of a prominent 2D band at 2639 cm^{-1} in Fig. 2b may be attributed to the formation of NRGO from GO. Fig 2c shows the Raman spectrum of $NiWO_4$-ZnO-NRGO ternary nanocomposite. Raman bands at 785 cm^{-1}, 901 cm^{-1} and 1038 cm^{-1} correspond to Raman active modes of $NiWO_4$.Bands at 115 cm^{-1}, 337 cm^{-1}, 410 cm^{-1}, 431 cm^{-1}, 535 cm^{-1}, 860 cm^{-1}, 1098 cm^{-1}, 1750 cm^{-1}, 2275 cm^{-1} and 2813 cm^{-1} correspond to the Raman active modes of ZnO [19]. Peaks at 1379 cm^{-1} (D mode); 1609 cm^{-1} (G mode) with I_D/I_G ratio 1.10 and 2D band at 2639 cm^{-1} with I_{2D}/I_G ratio as 1.06 correspond to presence of double layered NRGO with defects in the ternary composite. The change in the value of Raman frequencies of D and G band and increased value of I_D/I_G ratio in the composite may be due to the interaction between the NRGO sheets and the semiconductor particles.

3.3 Morphology Studies

The structural morphology of the as-synthesized nanocomposites was imaged by electron microscopy. Fig. 3a indicates the FESEM image of the $NiWO_4$-ZnO-NRGO ternary nanocomposite of the ZnO nanoparticles with the ball like shape and $NiWO_4$ sphere was anchored on the surface of the NRGO. In addition, statistics on the structural morphology of the nanocomposites, TEM and HRTEM were also imaged. Fig. 3b suggests the TEM image of the $NiWO_4$-ZnO-NRGO ternary nanocomposites at which certainly observed the sphere like $NiWO_4$ and ball like ZnO nanoparticles was uniformly distributed into the 2D sheet-like morphology of NRGO sheets. Further, Fig. 3cshows the interface between $NiWO_4$, ZnO and NRGO in $NiWO_4$-0.01M ZnO-2.5% NRGO ternary nanocomposite. The obtained lattice fringes of 0.15 nm correspond to the (111) plane of $NiWO_4$ and that of 0.283 nm correspond to the (100) plane of ZnO.

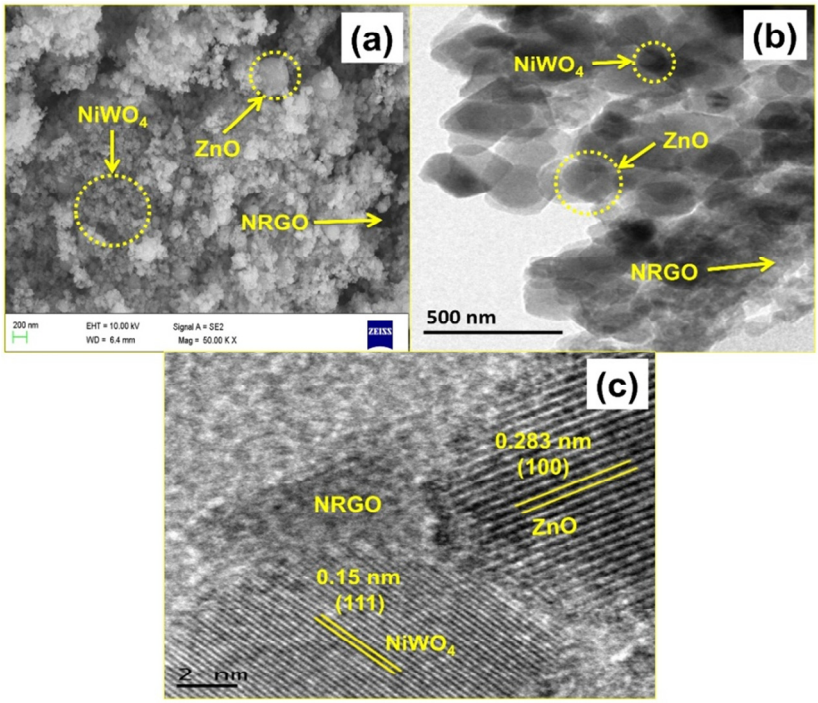

Fig. 3. (a) FESEM, (b) TEM and (c) HRTEM images of $NiWO_4$-ZnO-NRGO ternary nanocomposites.

3.4 XPS Studies

The high-resolution XPS spectrum of $NiWO_4$-ZnO-NRGO nanocomposites is shown in Fig. 4.The binding energy positions in the XPS spectrum were calibrated with C *1s* at 284.8 eV. Fig. 4a shows the C *1s* spectra which can be deconvoluted into five peaks at 284.5 eV (C-C/C=C), 285.5 eV (C-N), 286.1 eV (C-O) and 287.2 eV (C=O), respectively [14]. Fig. 4b reveals the N *1s* spectra which can be deconvoluted into four peaks at 398.4 eV (pyridinic-N), 399.4 eV (pyrrolic-N), 400.8 eV (graphitic-N) and 402.4 eV (pyridine-N-oxide), respectively [14]. Fig. 4c depicts Ni *2p* spectra deconvoluted into six peaks located at 855.9 eV, 857.7 eV (satellite), 861.6 eV which belongs to Ni $2p_{3/2}$ and 873.6 eV, 875.4 eV (satellite), 879.5 eV which belongs to the Ni $2p_{1/2}$, respectively [10].Fig. 4d shows the W *4f* spectra deconvoluted into four peaks corresponding to W $4f_{7/2}$ (34.8 eV and its satellite 35.4 eV) and W $4f_{5/2}$ (36.9 eV and its satellite 37.5 eV), respectively [17]. Fig. 4e shows the Zn *2p* spectra deconvoluted into four peaks placed at 1018.1 eV, 1019.6 eV (satellite) which belongs to Zn $2p_{3/2}$ and 1041.1 eV, 1042.5 eV (satellite) belongs to the Zn $2p_{1/2}$, respectively [17]. Fig. 4f reveals O *1s* spectra deconvoluted into three peaks at 531.2 eV, 532.2 eV and 533.1 eV related to ZnO, $NiWO_4$ and H-O-H bonds, respectively [15].

3.5 Optical absorbance analysis

The optical properties of the as-synthesized nanocomposites are studied by DRS. The absorption of $NiWO_4$-ZnO-NRGO (Fig. 5a) is high in comparison to $NiWO_4$-NRGOand $NiWO_4$. The optical energy band gap (Fig. 5b) of the nanocomposites was measured using the Tauc relation, $\alpha h\nu = A\ (h\nu - E_g)^{n/2}$, where α, h, ν, E_g and n denote the absorption coefficient, Planck's constant, the velocity of light, energy band gap and the type of transition of the semiconductor. The value of n is 1 and 4 for direct and indirect band gap. The present results correspond to the direct band gap as n=1 [14, 15]. The obtained band gap energy values of $NiWO_4$, $NiWO_4$-NRGO and $NiWO_4$-ZnO-NRGO are 3.10 eV, 2.42 eV and 2.27 eV, respectively. Furthermore, the band gap energy of the ternary nanocomposite is appreciably reduced in comparison to the pure $NiWO_4$. This may be due to the synergic effect of the composite components, ZnO and NRGO.

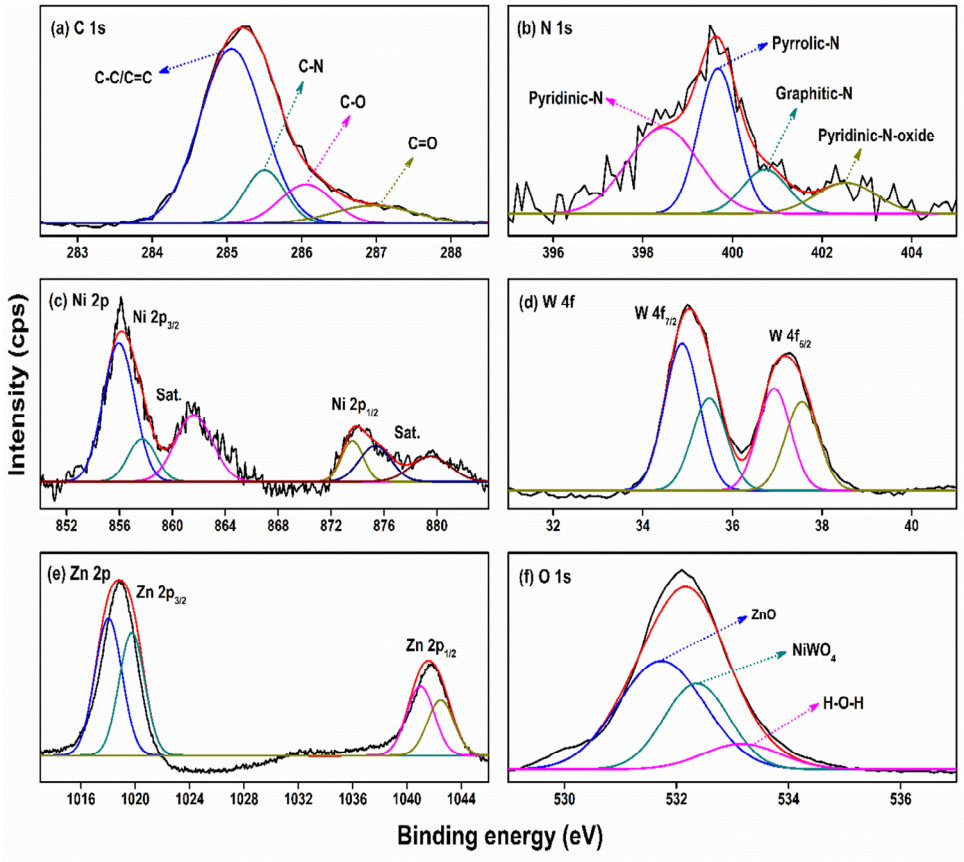

Fig. 4. High-resolution XPS spectra of $NiWO_4$-ZnO-NRGO (a) C *1s*, (b) N *1s*, (c) Ni *2p*, (d) W *4f*, (e) Zn *2p* and (f) O *1s*.

3.6 Photoluminescence analysis

An efficient photocatalyst should have very less recombination rate of photogenerated electron hole pair. The recombination of photogenerated electron-holes and charge separation in the ternary nanocomposite were investigated through PL emission spectrum [15] as shown in Fig. 5c. An intense PL peak corresponds to faster recombination rate of photo generated electron-hole pairs. All the synthesized materials exhibited a broad emission peak in the visible region starting from 420 nm to 700 nm with the excitation wavelength of about 400 nm. Pure $NiWO_4$ showed an intense broad peak around 520 nm indicating rapid recombination of charge carriers. Introduction of NRGO led to slight decrease in PL intensity. The higher conductivity of the NRGO sheet matrix facilitates smooth electron transport and hence results in the increased separation of electron hole pairs. Further, when ZnO is introduced, the PL spectrum of $NiWO_4$-ZnO-NRGO nanocomposite exhibits very less intensity. This can be ascribed to the contribution of ZnO towards further separation of electron hole pairs. In the ternary composite, electrons are excited from VB to CB of ZnO and then immediately transported to the CB of $NiWO_4$ due to favorable energy level difference. From CB of $NiWO_4$ electrons would get transported through NRGO network due to the high conductivity of NRGO. Thus, the entire process results in an efficient and enhanced separation of electron hole pairs and leads to appreciable decrease in the PL intensity in $NiWO_4$-ZnO-NRGO nanocomposite [14].

3.7 Photocatalytic activity

The photocatalytic activity of $NiWO_4$-ZnO-NRGO ternary nanocomposite was assessed by the photocatalytic dye degradation of MB using the visible light source. The results were compared with the component materials NRGO,

ZnO, $NiWO_4$, ZnO-NRGO and $NiWO_4$-NRGO (Fig. 6a). Blank test (control) was performed without the addition of nanocomposite and there was no noticeable degradation indicating that the photolysis of MB was negligible.

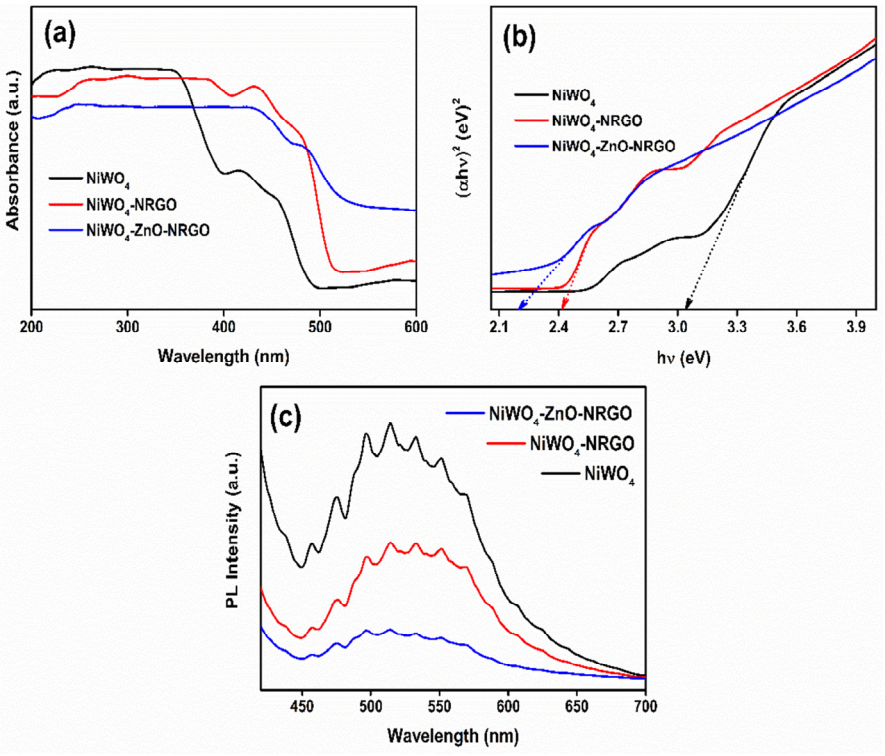

Fig. 5. (a) UV-Vis spectra, (b) band gap plots and (c) PL spectra of ZnO, $NiWO_4$, ZnO-NRGO, $NiWO_4$-NRGO and $NiWO_4$-ZnO-NRGO ternary nanocomposites.

The photocatalytic dye degradation efficiency of MB solutions in the presence of NRGO, ZnO, $NiWO_4$, ZnO-NRGO, $NiWO_4$-NRGO and$NiWO_4$-ZnO-NRGO were about 17.35 %, 35.66 %, 28.55 %,53.03 %, 73.89 % and 99.27 %, under visible light irradiation in time duration of 120 minutes. The obtained results show that the $NiWO_4$-ZnO-NRGO ternary nanocomposite have excellent photocatalytic degradation efficiency than that of pure $NiWO_4$, and that the photocatalytic degradation efficiency of the $NiWO_4$-ZnO-NRGO is significantly enhanced due to the synergic effect of the $NiWO_4$, ZnO and NRGO [15].

The as-prepared nanocomposite followed the first order kinetics [18] of photocatalytic degradation of MB solution as given in equation (2)

$$ln\ (C/C_o) = -kt \qquad \text{---------- (2)}$$

where, C is the initial concentration of the MB dye, C_o is the concentration of the MB at the irradiation time (t) and k is the first order rate constant. The rate constant k values were calculated from the slope of the straight line (Fig. 6b). Inset of Fig. 6b shows that the rate constant values of the different nanocomposites. The first order rate constants of ternary composite indicate 9 times more photocatalytic efficiency than the pure $NiWO_4$, respectively. To determine the active species involved in photodegradation and to find out the mechanism, trapping experiments were carried using scavenging agents (Fig. 6c) such as, benzoquinone (BQ, a quencher of $O_2^{\cdot-}$), potassium iodide (KI, a quencher of h^+), silver nitrate ($AgNO_3$, a quencher of e^-) and ternary butanol (TBA, a quencher of $OH^{\cdot}$).

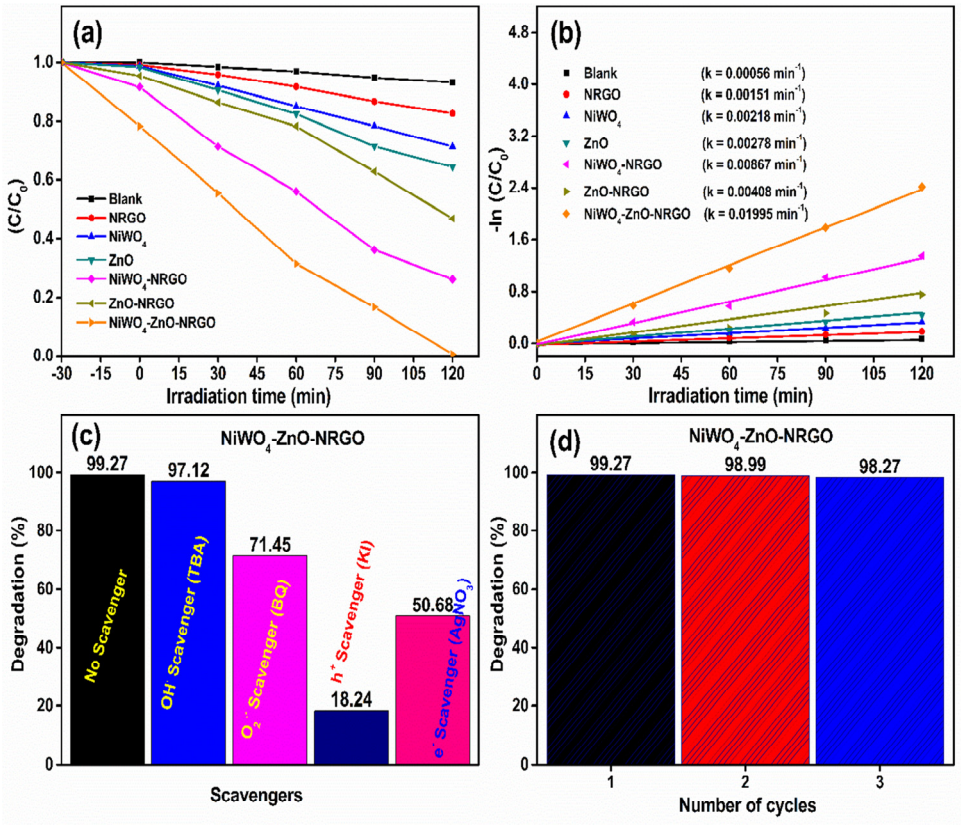

Fig. 6. (a) Degradation rate, (b) first order kinetics plot, (c) effects of different scavengers and (d) Reusability of the photodegradation of MB using $NiWO_4$-ZnO-NRGO ternary composites under visible light irradiation.

Addition of TBA caused only a small decrease in efficiency (97.12 %) which meant hydroxyl radical was not the active species. But addition of KI, $AgNO_3$ and BQ caused dramatic decrease in the efficiency 18.24 %, 50.68 % and 71.45 % respectively. Based on these results the following mechanism is proposed.

$$ZnO + hv \rightarrow ZnO(e^-_{CB} + h^+_{VB}) \quad \text{---------- --- (3)}$$

$$ZnO\ (e^-_{CB}) + NiWO_4 \rightarrow ZnO + NiWO_4\ (e^-_{CB}) \quad \text{---------- --- (4)}$$

$$NiWO_4\ (e^-_{CB}) + O_2 \rightarrow NiWO_4 + O_2^- \quad \text{----------(5)}$$

$$ZnO\ (h^+_{VB}) + MB \rightarrow CO_2 + H_2O + Inorganic\ species \quad \text{----------(6)}$$

where e^-_{CB} is the electron in the conduction band and h^+_{VB} is the hole in the valence band, respectively.

The durability of the ternary nanocomposites was additionally investigated and as shown in the Fig. 6d. It was seen that even after 3 consecutive cycles the photocatalytic activity of nanocomposite showed only a small reduction in efficiency from 99.27 % to 98.27 %, which is negligible. The results indicate that the ternary composites have sufficient stability to be used in environmental applications.

4. Conclusions

In this work, $NiWO_4$-ZnO-NRGO ternary composites were successfully prepared by microwave irradiation method and its characterization by XRD, Raman, FESEM, TEM, HRTEM, XPS, PL and UV-Visible spectroscopy. The as-synthesized nanocomposite was studied by photocatalytic properties using MB under the visible light source. The observed results show that photodegradation efficiency of $NiWO_4$-ZnO-NRGO was approximately 9 times higher than $NiWO_4$ and it showed high stability even after 3 cycles. The trapping experiment suggested the photogenerated holes were the active species involved in the photocatalytic reactions. On the basis of the experimental results, the possible photodegradation mechanism was proposed.Therefore, these new $NiWO_4$-ZnO-NRGO ternary compositesnanocomposites may be suitable materials for various environmental applications.

Acknowledgments

MJSM is thankful to the National Institute of Technology Karnataka, Surathakal, India for the award of a research fellowship.

References

[1] D. Chen, H. Zhu, S. Yang, N. Li, Q. Xu, H. Li, J. He, J. Lu, Adv. Mater. 28 (2016) 10443-10458.
[2] M.M.J. Sadiq, A.S. Nesaraj, J. Nanostruct. Chem. 5 (2014) 45-54.
[3] A.S. Bhatt, D.K. Bhat, Polym. Bull. 68 (2012) 253-261.
[4] M. Selvakumar, D.K. Bhat, Appl. Surf. Sci. 263 (2012) 236-241.
[5] A.S. Bhatt, D.K. Bhat, M.S. Santosh, J. Appl. Polym. Sci. 119 (2011) 968-972.
[6] A.S. Bhatt, D.K. Bhat, Mater. Sci. Engg. B 177 (2012) 127-131.
[7] M.M.J. Sadiq, D.K. Bhat,AIMS Mater. Sci. 4 (2017) 487-502.
[8] M.M.J. Sadiq, U.S. Shenoy, D.K. Bhat,Adv. Sci. Eng. Med. 9 (2017) 115-121.
[9] B. Subramanya, D.K. Bhat, S.U. Shenoy, Y. Ullal, A.C. Hegde, Int. J. Hydrogen Energy 40 (2015) 10453-10462.
[10] B. Subramanya, Y. Ullal, S.U. Shenoy, D.K. Bhat, A.C. Hegde, RSC Adv. 5 (2015) 47398-47407.
[11] B. Subramanya, D. K. Bhat, J. Power Sources 275 (2015) 90-98.
[12] B. Subramanya, D.K. Bhat, New J. Chem. 39 (2014) 420-430.
[13] H. Zhang, X. Fan, X. Quan, S. Chen, H.Yu, Environ. Sci. Technol. 45 (2011) 5731-5736.
[14] M.M.J. Sadiq, U.S. Shenoy, D.K. Bhat, Mat. Today. Chem. 4 (2017) 133-141.
[15] M.M.J. Sadiq, U.S. Shenoy, D.K. Bhat, RSC Adv. 6 (2016) 61821-61829.
[16] H. Chang, H. Wu, Energy Environ. Sci. 6 (2013) 3483-3507.
[17] M.M. J. Sadiq, D.K. Bhat, Ind. Eng. Chem. Res. 55 (2016) 7267-7272.
[18] M.M.J. Sadiq, D.K. Bhat, AIMS Mater. Sci. 4 (2017) 158-171.
[19] D.K. Bhat, Nanoscale Res. Lett. 3 (2008) 31-35.
[20] A.H.Keihan, R.Hosseinzadeh, M.Farhadian, H.Kooshki, G. Hosseinzadeh, RSC Adv. 6 (2016) 83673-83687.
[21] Q. Xiang, D. Lang, T. Shen, F. Liu, Appl. Cat. B: Environ. 162 (2015) 196-203.
[22] G. Chen, H. Guan, C. Dong, X. Xiao, Y. Wang, J. Phys. Chem. Solids 98 (2016) 209-219.
[23] Y. Ma, Y. Guo, H. Jiang, D. Qu, J. Liu, W. Kang, Y. Yi, W. Zhang, J. Shi, Z. Han, New J. Chem. 39, (2015) 5612-5620.